NANO LETTERS

LETTER

pubs.acs.org/NanoLett

Background-Free Detection of Single 5 nm Nanoparticles through Interferometric Cross-Polarization Microscopy

Xin Hong,[†,‡] Erik M. P. H. van Dijk,[§] Simon R. Hall,[∥] Jörg B. Götte,[†] Niek. F. van Hulst,[⊥] and Henkjan Gersen*[,†]

[†]Nanophysics and Soft Matter Group, H. H. Wills Physics Laboratory, University of Bristol, BS8 1TL, United Kingdom

[‡]College of Precision Instrument & Optoelectronics Engineering, Tianjin University, Tianjin, China

[§]Faculty of Science and Technology, University of Twente, 7500 AE Enschede, The Netherlands

[∥]Inorganic and Materials Chemistry, University of Bristol, BS8 1TS, United Kingdom

[⊥]ICFO—Institut de Ciencies Fotoniques, Mediterranean Technology Park, 08860 Castelldefels (Barcelona), Spain

ABSTRACT: Metal nanoparticles play a key role in sensing and imaging. Here we demonstrate the detection of metal particles down to 5 nm in size with a signal-to-noise ratio of ~7 using interferometric cross-polarization microscopy at ultralow excitation powers (~1 μW) compatible with single molecule detection. The method is background-free and induces no heating as it operates far from plasmonic resonance. The combination of unlimited observation time and protein-sized metal nanoparticles has great potential for biophysical applications.

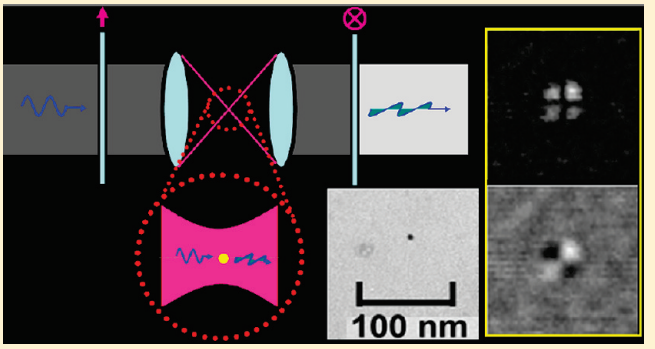

KEYWORDS: Background-free detection, gold nanoparticles, polarization microscopy, crossed polarizers, heterodyne detection, interferometry

Precise control of size and shape of materials on nanometer length scale is developing rapidly and does enable the engineering of optical responses that are fundamentally different from those found in the bulk material they are made of. Current nanofabrication control has already opened up completely new areas of fundamental research such as plasmonics,[1] negative-index materials,[2] and photonic crystal structures.[3,4] At the same time such nanostructures are finding interesting applications in applied nanoscience; i.e., engineering the shape and size of metallic nanoparticles provides superior alternatives to fluorescent markers with unique and highly desirable optical properties such as high brightness, biocompability, no blinking, and an unlimited observation time. The tunability of the optical response relies on the fact that optical properties of individual nanostructures are dependent strongly on their size, shape, material, and their local environment. In fact plasmonic sensing with metal particles exploits exactly this dependence. However intrinsic variations in these properties from object to object do lead to strong variations in their optical response. A conventional optical experiment, which averages over many individual nanostructures, will make a qualitative comparison with theoretical models thus complex through the need to include various statistical effects. As a result the development of techniques that can detect and characterize the optical response of a single nanostructure is of central interest to both fundamental and applied nanoscience.

In this paper we demonstrate a novel approach to detect nanoparticles a few nanometers in size using a single continuous wave laser far from the plasmon resonance with an excellent signal-to-noise ratio that allows the study of the optical properties of individual nanostructures. Moreover we realized such sensitive detection at the very low excitation intensities (~1.0 μW) needed for single molecule fluorescence and bioimaging experiments as metallic nanoparticles can be easily attached to biomolecules providing markers with high brightness, biocompatibility, no blinking or bleaching, and thus unlimited lifetime. As a result new experimental avenues are opened up for colocalization experiments as well as for exploration of interaction between fluorescent emitters and (metal) nanoparticles.[5]

The challenge in detecting single nanosized particles is comparable to the challenge of finding a needle in a haystack. Due to the small cross section of the particle, only a small fraction of the incident light will impinge on the particle while the rest of the excitation light passes the object unperturbed resulting in a large background from which the signal from the particle itself must be retrieved. To overcome this problem, one has either to increase the ratio between the cross section of the nanoparticle and the illumination area, which can be done by exciting at the plasmon

Received: September 30, 2010
Revised: December 13, 2010
Published: January 4, 2011

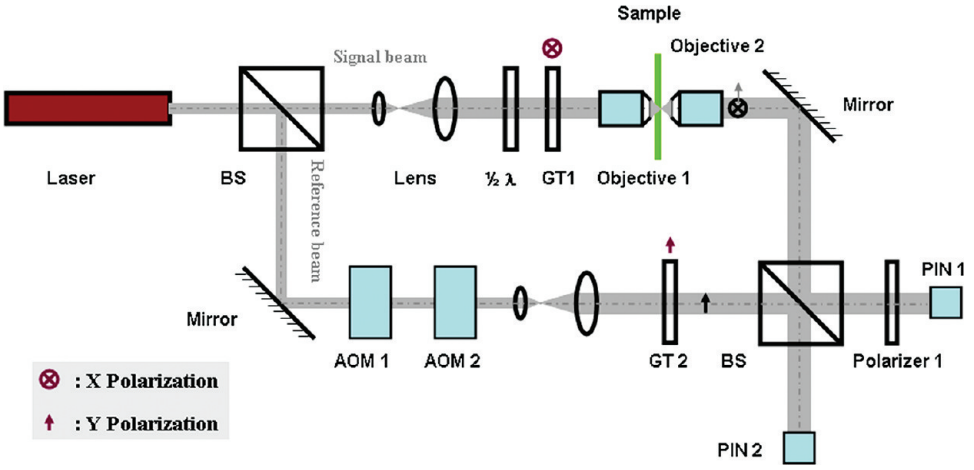

Figure 1. Schematic diagram of an interferometric cross-polarization microscope for detecting single nanoparticles. Linear polarized light is split by a beamsplitter into a signal and reference branch that are adjusted to *x*- and *y*-polarized light, respectively. Light in the signal-branch is focused onto the sample by a high-NA objective that induces a partial polarization conversion from *x* into *y* polarization in the focus of the objective. Only when a small scattering object is in focus will these *y*-polarized field components be scattered and collected by a second objective. When the signal beam is overlapped with the reference beam, only these weak *y*-polarized field components will interfere as the reference is orthogonal in polarization to the excitation. This leads to a shot-noise limited background-free detection method of single nanoparticles.

wavelength or by devising a method that efficiently separates the background from the relevant signal. This general principle underlies the different ways in which optical detection of small nanoparticles has been achieved.[6−11] In all approaches in which the detection wavelength is the same as the one used for excitation (or probing), the method relies on interference of the scattered wave with a reference wave as recently reviewed.[12] The main advantage of using interference is the increased sensitivity as the signal varies only with the third power of the particle size in contrast to Rayleigh scattering which scales with the sixth power limiting it to detection of particles larger than ∼30 nm in diameter. One of the most sensitive of these methods, photothermal heterodyne imaging pioneered by Berciaud et al.,[9] has demonstrated detection of particles of 5 nm diameter with a signal-to-noise ratio of about 10 at excitation intensities of 500 μW with an integration time of 10 ms.[13] Questions have however been raised on how the local heating of the nanoparticles with the high power laser used in this method will influence the behavior of the object under study in certain applications. For instance, proteins easily denature when the temperature is raised, an effect that would severely hamper the application of this method to living cells. Moreover this method measures a combination of the particle response itself with the heat-induced change in local refractive index around the particle. Hence one does not measure the optical properties of the particle itself directly. An alternative method pioneered by Arbouet et al.[6] that is capable of detecting the optical properties of metal particles itself has also demonstrated detection of single metal nanoparticles down to 5 nm using modulation of the particle position. Yet it appears that the relatively slow mechanical motion that can be imposed limits both the acquisition speed and sensitivity in this approach. Unfortunately the lack of experimental details on the used integration times in the papers using this method[6,14] makes a direct comparison difficult.

A technique that has been very successful in detecting larger objects (>30 nm) is based on a cross-polarized detection scheme which exploits the change in polarization direction of the light scattered from a nanoparticle.[15] This effect arises because of the fact that a high NA objective induces a partial conversion of the polarization of the electric field in the focus which is probed efficiently by the nanoparticle. Nanoparticles larger than the ones investigated in this paper will simultaneously induce depolarization of the light itself, but this effect is not significant for the sizes measured here.[16] The resulting depolarization signal is however very weak and extinction ratios of polarizers are finite, which limits the observation to particles >30 nm in diameter. Here we show that this detection limit can be overcome by interfering the signal with a strong reference to optically amplify the signal of interest. The resulting interference signal on the detector is then proportional to the product of reference (E_{ref}) and signal (E_{signal}) field leading to a detection sensitivity only limited by the shot noise of the actual optical signal from the nanoparticle for suitably chosen power ($E_{ref} \gg E_{signal}$) in the reference branch.[17] Moreover the obtainable background reduction is no longer limited by the finite extinction ratio of the crossed polarizers because we exploit coherent detection of fields and the coherent image formation in the confocal scanning microscope allows infinite extinction ratios to be obtained even for nonperfect polarizers, as shown by Wilson et al.[18] Thus our approach is background-free. Alternatively this can be understood from the fact that the unperturbed excitation light has an orthogonal polarization with respect to the reference and hence will not interfere with the signal from the particle. The only signal that is detected is the interference of the reference branch with light that is scattered by the nanoparticle and hence free of background signal.

The essence of the setup needed to implement the above detection principle for small nanoparticles is described in the functional equivalent in Figure 1. Linearly polarized laserlight (λ = 632.8 nm or λ = 532 nm) is split in a signal and reference beam, respectively, by a 50−50 beam splitter. The signal beam is enlarged using a beam expander and passed through a half waveplate and a Glan Taylor polarizer (GTP) to be able to rotate the polarization in the signal branch in an arbitrary direction to assist during alignment. During the measurement these two components are optimized to ensure that the light in

dx.doi.org/10.1021/nl1034489 |*Nano Lett.* 2011, 11, 541–547

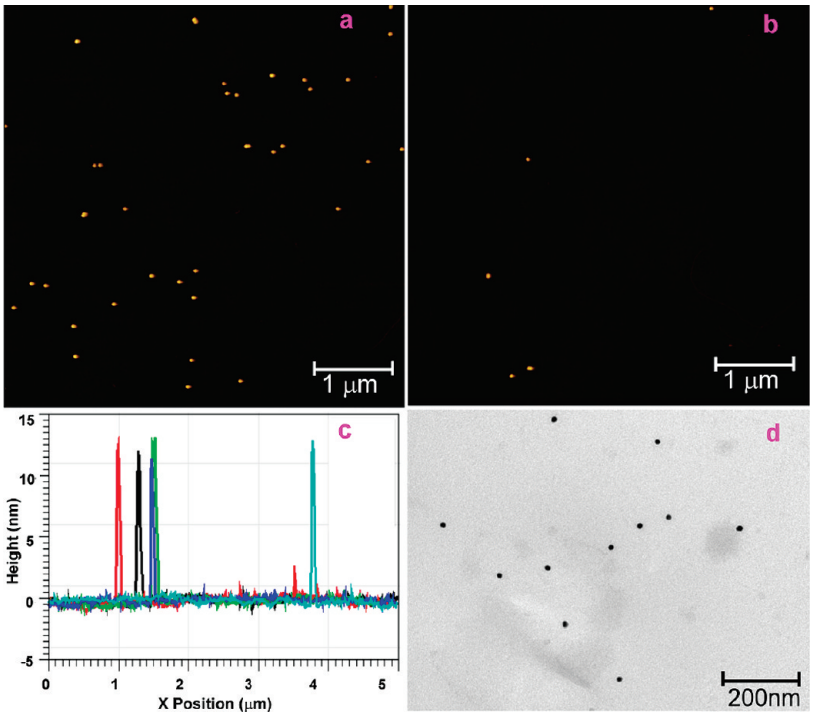

Figure 2. Concentration-dependent surface coverage density of gold nanoparticles as studied with AFM and TEM. Gold nanoparticles are deposited onto the cover glass and linked by poly-L-lysine. (a) 15 nm gold nanoparticles from a solution with a concentration of 4.65×10^{-11} mol/L; (b) 15 nm gold nanoparticles with the concentration of 4.65×10^{-12} mol/L. (c) Line scans across a number of particles demonstrating that the particles are in fact 13 ± 2 nm in size. From these images it is clear that the nanoparticles do not aggregate and are on average separated by >1 μm for the concentration used in (b), proving that we are imaging single nanoparticles of 13 ± 2 nm. (d) Typical TEM image of these 15 nm particles spin coated in PVA, as used in the optical experiments displayed in Figures 3 and 4, directly on a TEM grid further corroborating that we are detecting single nanoparticles.

the signal branch is *x*-polarized and orthogonal to the light in the reference branch. Next the light is focused onto the sample by an oil immersion objective (1.3 NA). A second air objective (0.9 NA) is positioned such that the focus coincides with that of the first objective and collects and collimates the transmitted light. The light in the reference branch is passed through two acoustic—optical modulators (AOM) to generate a difference frequency of 70 kHz with respect to the light in the signal branch which enables us to perform heterodyne detection as well as to retrieve the amplitude and phase of the light scattered by the nanoparticle; a technique described in more detail elsewhere.[19] This light in the reference branch is subsequently expanded using a beam expander and passed through a GTP to ensure that linear *y*-polarized light is obtained. Finally the light from the signal and reference branch are recombined using a second 50—50 beamsplitter. The optical interference signal is detected using two silicon photodiodes at both of the outputs of the last beamsplitter. After preamplification each of the detector outputs is sent to a lock-in amplifier to demodulate the signal. To do this a polarizer is placed in front of detector 1 with its fast axis under 45° with respect to the *x* axis, so that the projection of the light for the two branches onto the fast axis of the polarizer will generate interference between the excitation light in the signal and reference branch, which can be used to generate the 70 kHz reference signal that is needed by the lock-in amplifier to perform the demodulation. The second photodiode detects the actual interference between the signal scattered by the nanoparticle and the light in the reference branch. During initial alignment, with no nanoparticles present in the focus of the objectives, the signal on the second detector is minimized after optimizing the overlap between the two beams by adjusting the setting of the waveplate and GTP in the signal branch and hence ensuring that the polarization direction of the beams in signal and reference branch are orthogonal.

Besides a few orders of magnitude enhancement of the optical signal as a result of detecting fields, this new setup has the important advantage that it is capable to selectively measure both *amplitude* and *phase* of the field that has undergone a polarization change due to the presence of a small scattering object. Here we demonstrate the combined advantage by imaging gold nanoparticles down to 5 nm deposited on a glass substrate. First we ensure that on average we only have a single nanoparticle within the focal area of the objectives; i.e., on average individual particles need to be separated by a distance larger than the diameter of the airy disk (~550 nm). To this end the surface coverage of gold nanoparticles was first studied using a combination of atomic force microscopy (AFM) and transmission electron microscopy (TEM). After diluting the solution containing ~15 nm sized gold nanoparticles, as purchased from BBI, the nanoparticles were attached to a cover glass by poly-L-lysine using well-established procedures. Figure 2, shows a typical scan of a randomly chosen $5\ \mu m \times 5\ \mu m$ area for these particles. Figure 2a shows an image deposited from a solution with a concentration of 4.65×10^{-11} mol/L in which it is clearly visible that all of the nanoparticles are well separated and do not aggregate. Figure 2b shows a similar AFM image as obtained after depositing a 10 times further diluted solution, showing particles separated from each other by a distance of more than 1 μm, resulting in a surface density

dx.doi.org/10.1021/nl1034489 |*Nano Lett.* 2011, 11, 541–547

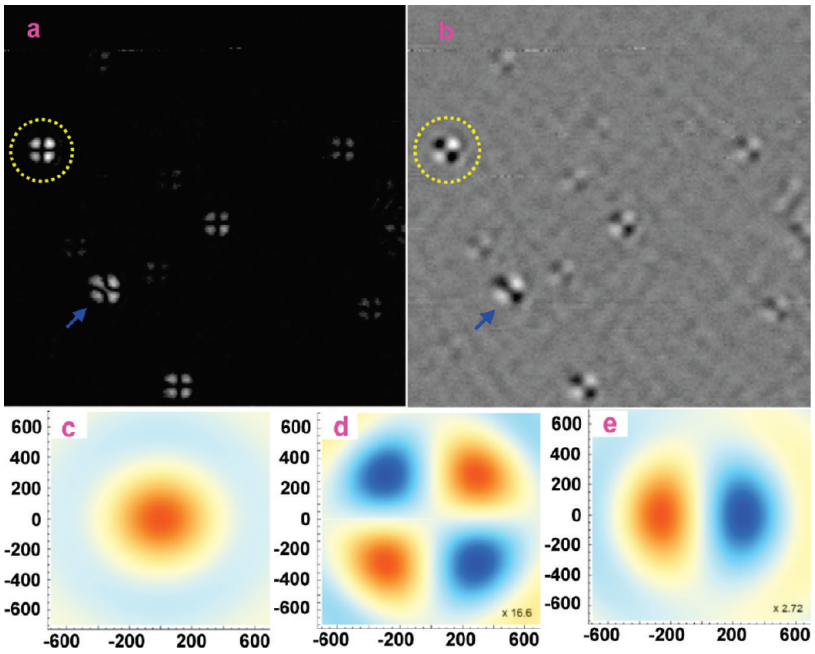

Figure 3. Interferometric cross-polarization images of 13 ± 2 nm gold nanoparticles from a concentration of 4.65×10^{-12} mol/L spin coated in PVA (image size, 10 μm × 10 μm; integration time, 3 ms; λ = 632.8 nm; power on the sample 0.8 μW). (a) The optical amplitude of the scattered light. (b) The optical phase difference with respect to the light in the reference branch. The yellow circle highlights the typical response for a single nanoparticle while the blue arrow indicates a slightly different response indicative for two closely spaced nanoparticles. (c−e) The calculated E_x, E_y, and E_z field components, respectively, in a 1.3 NA objective in which red is positive and blue is negative. The similarity of the detected clover-leaf pattern as visible in (a) demonstrates that in our approach a subwavelength scatterer selectively probes the E_y field in the focus of the objective.

that is sufficiently decreased to ensure that on average we only have one single particle within the focal spot of our objective. Note that for this concentration, as used in the subsequent optical experiments, incidentally particles can be closer together than 500 nm, an example of which is visible in the bottom left corner of Figure 2b. These AFM images furthermore show that the size of the imaged nanoparticles is 13 ± 2 nm, slightly below the specified size of 15 nm, as demonstrated by depicting a number of line scans through the center of particles as depicted in Figure 2c. TEM data shown in Figure 2d, on samples with a high concentration of nanoparticles in PVA (the polymer used in the optical experiments presented in Figures 3 and 4) spin coated directly onto a TEM grid, further corroborate that we are indeed looking at individual nanoparticles in our experiments. Panels a and b of Figure 3 show the measured optical amplitude and phase image, respectively, with a λ = 632.8 nm excitation as obtained for these ∼15 nm sized gold nanoparticles for coverages of nanoparticles similar to those in Figure 2b for the particles embedded in a spin-coated PVA layer. The observed density when imaging larger areas than shown here is in excellent agreement with those retrieved from the AFM images for the same concentration of the solution. In the amplitude image individual nanoparticles show up in the form of a clover-leaf pattern, as highlighted by the yellow circle, instead of a round pattern in which there is a relative phase difference of π between lobes as visible in Figure 3b. Although this pattern at first might appear surprising, it is relatively easy to understand why we observe this pattern as explained below.

The scattering of a homogeneous sphere has a rigorous solution and was derived by Mie in 1908.[20] For the limiting case in which the particle is much smaller than the wavelength of light, as is the case here, this theory shows that in this regime a scattering particle is equivalent to that of an oscillating dipole with a dipole moment parallel with the incoming electric field.[21] As a result the nanoparticle maps out the complex field distribution of a high NA objective similar to experiment using single fluorescent molecules to map out focal distributions.[22,23] In our experiment x-polarized light is focused onto the sample by a 1.3 NA microscopy objective and about 12% of the amplitude of this light will be converted into y-polarized light while 22% is converted into z polarization with the distributions as shown in Figure 3c−e. When the nanoparticles are brought into the y-polarized field components, a dipole parallel to the local field will be induced in the nanoparticle that will lead to a y-polarized radiation that is collected by the top objective and can be detected in the far-field. In our case we only detect light polarized along the y direction as the x direction is orthogonal to the polarization in the reference branch and hence does not yield an interference signal. As a result the small size nanoparticles studied in this paper effectively map out the y component of the focus distribution as is clearly demonstrated by the similarity of the clover-leaf pattern observed in our experiments with the simulated focal distribution in a high NA objective displayed in Figure 3d.

Clear differences in measured signal strength can be seen for the different particles visible in the optical amplitude image displayed in Figure 3a. We tentatively attribute this to the fact that we are imaging a spread of sizes (13 ± 2 nm) as is apparent from the height scan displayed in Figure 2c. The observation that such a small size difference has such a dramatic effect on the strength of the optical signal in the images can be understood from the fact that the strength of the scattered field scales as r^3 (with r the radius of the particle) for a scatterer much smaller than the wavelength as follows directly from Mie's theory.

dx.doi.org/10.1021/nl1034489 |*Nano Lett.* 2011, 11, 541–547

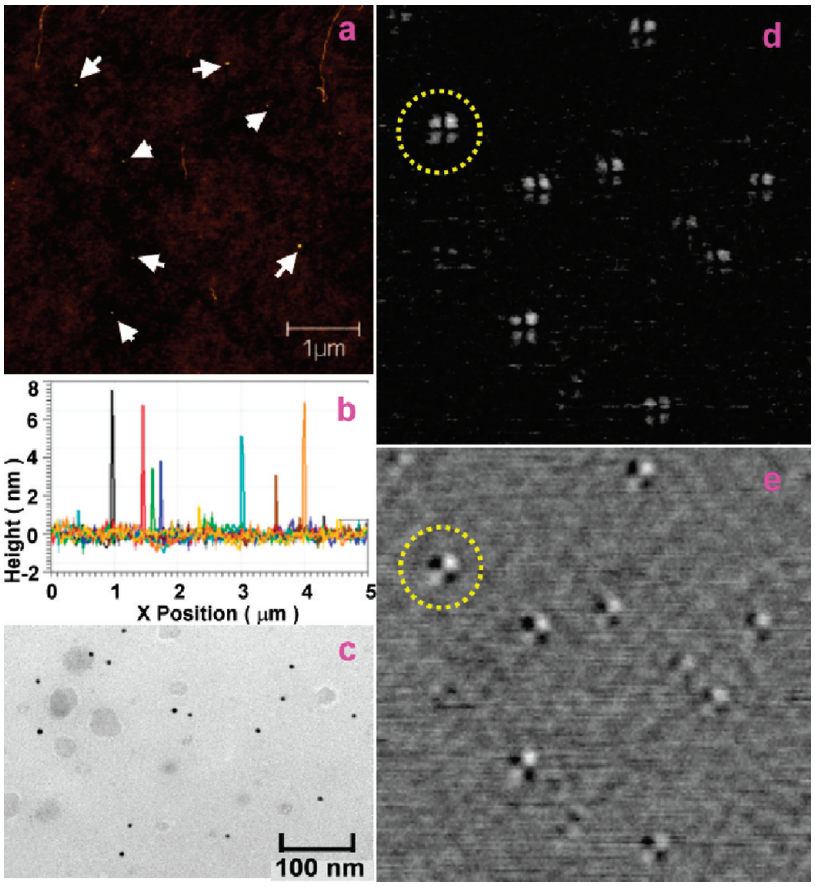

Figure 4. (a) AFM image of 5 nm gold nanoparticles linked by poly-L-lysine for a concentration of 2.77×10^{-11} mol/L. (b) Line scans across a number of particles demonstrating that these particles are 5 ± 2 nm in size. (c) TEM of these 5 nm particles into PVA spin coated directly onto a TEM grid. (d, e) The optical amplitude and phase, respectively, for a concentration of 2.77×10^{-11} mol/L spin coated in PVA of the light scattered by these 5 nm gold nanoparticles. Note that the sample preparation for these optical images is the same as used in preparing the TEM image. (image size, 10 μm × 10 μm; integration time, 3 ms; λ = 632.8 nm; power on the sample, 0.8 μW).

Moreover, when looking in slightly more detail at the patterns seen in the image, it is clear that one of the phase patterns, as highlighted by the blue arrow, shows a slightly different pattern with respect to the others. We tentatively attribute this to imaging of two particles that are too close together which would be consistent with the densities seen in the AFM coverage experiments as observance of such different phase patterns in our optical images is rare.

The sensitivity of our technique is particularly demonstrated in experiments on commercially available 5 nm gold particles (BBI, U.K.) the results of which are presented in Figure 4. In this Figure 4a shows an AFM image of 5 nm gold nanoparticles in which the background roughness visible arises due to the ~1 nm thick poly-L-lysine layer covering the glass surface. The particles in this case show a size distribution of 5 ± 2 nm as shown in Figure 4b by aggregating a number of line scans across particles. The typical separation distance between particles is again more than 1 μm, and TEM on particles spin coated in PVA (the polymer used in the optical experiment presented in Figure 4), again corroborates that we are looking at the optical response of individual nanoparticles in Figure 4. For these particles the optical amplitude and phase images obtained with λ = 632.8 nm are shown in panels d and e of Figure 4, respectively, showing the expected symmetric clover-leaf patterns also for these particles.

The presence of a plasmon resonance in metallic nanoparticles can be used to provide further evidence for the detection of metallic nanoparticles as the extinction cross section (σ_{ext}) is ~8 times larger at 532 nm than at 632.8 nm as, e.g., measured by Muskens et al. (see Figure 5 in ref 15) as the scattering of most dielectrics does not vary this strongly over this wavelength range. For this reason a sample with 5 nm gold nanoparticles attached to the cover glass by poly-L-lysine was imaged sequentially with wavelengths of λ = 632.8 nm (red) and λ = 532 nm (green) as displayed in panels a and b of Figure 5, respectively. These results have been obtained with an excitation power of 1.0 μW in the signal branch with power of 10.1 and 6.2 μW in the reference branch for red and green excitation, respectively. Both of these images show the same nanoparticles with an improved signal-to-noise ratio for excitation at λ = 532 nm as expected. This improved signal-to-noise can be seen even better in the line traces displayed in Figure 5c for the nanoparticle highlighted by the circle displayed in panels a and b of Figure 5 for red and green excitation, respectively, showing a signal-to-noise ratio of ~7 (red) and ~16 (green). Note that the ratio between the measured signals scales with $(\sigma_{green}/\sigma_{red})^{1/2}$ as we are measuring fields, not intensities. Correcting for the different powers in the reference branch shows that we measure a ratio for the extinction cross sections of $\sigma_{green}/\sigma_{red}$ equal to 8.1, which is in excellent agreement with the value measured by Muskens et al.[14] This

dx.doi.org/10.1021/nl1034489 |*Nano Lett.* 2011, 11, 541–547

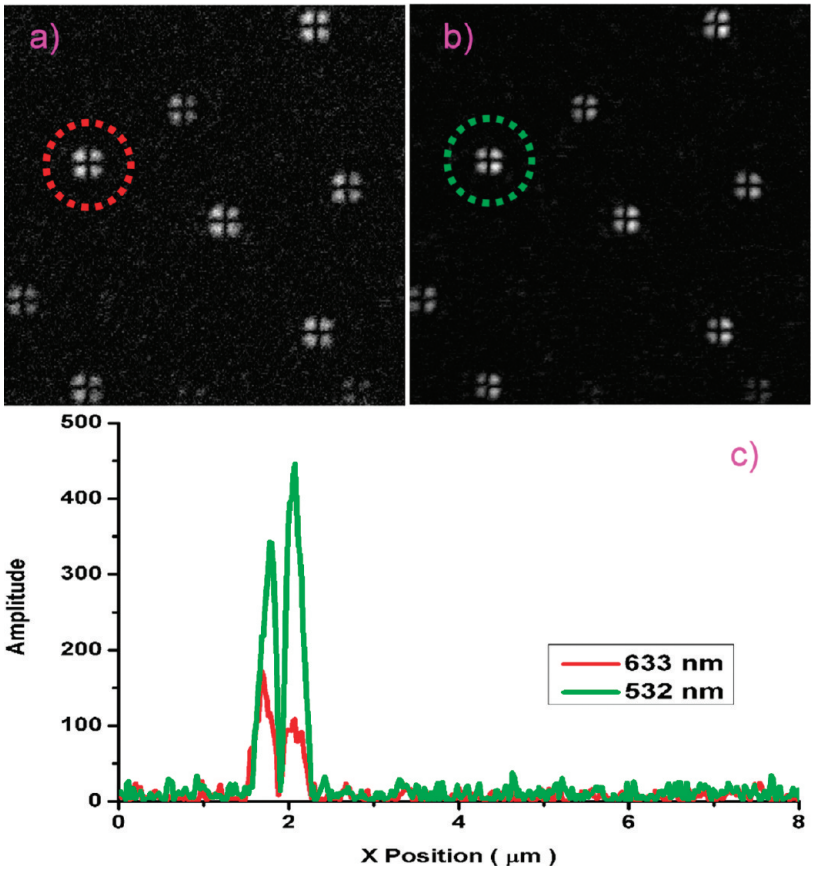

Figure 5. (a, b) Optical amplitude images of 5 nm gold nanoparticles linked by poly-L-lysine for a concentration of 2.77×10^{-11} mol/L for excitation at 632.8 and 532 nm, respectively. (c) Line traces through the signal of the same particle highlighted with the circle in (a) and (b) for excitation at 632.8 and 532 nm, respectively, showing that we obtain a signal-to-noise of ~7 (red) and ~16 (red) in these experiments with an integration time of 3 ms for particles of ~5 nm in size for laser powers that are 1.0 μW on the sample. This demonstrates that we can detect the same size nanoparticles with a comparable signal-to-noise as obtained with the photothermal heterodyne imaging approach but for excitation powers that are 2 orders of magnitude lower.

combined with the evidence that we have well-isolated particles on our samples as shown by both AFM and TEM proves that we are measuring individual metal nanoparticles down to 5 nm diameter. The varying strength of the amplitude signal in these images due to a spread in sizes unfortunately makes it difficult to exactly state to which size the line scans displayed in Figure 5 correspond, but it does demonstrate that we obtain a signal-to-noise of ~7 in these experiments with an integration time of 3 ms for particles of ~5 nm in size for laser powers that are 1.0 μW on the sample for excitation wavelengths far from the plasmon resonance. This demonstrates that we are able to detect the same size nanoparticles with a comparable signal-to-noise as obtained with the photothermal heterodyne imaging approach but for excitation powers that are 2 orders of magnitude lower. Our excellent signal-to-noise ratio for excitation powers compatible with single molecule fluorescence imaging enables further application in single molecule bioimaging in combination with fluorescence imaging. Moreover in contrast to the results obtained by photothermal heterodyne imaging, we operate far from the plasmon resonance to demonstrate the ability of this technique to probe optical properties of nanometer sized properties over a much broader spectral range potentially allowing us to measure the spectral response of individual nanostructures. We expect that improvement of the experimental setup would further improve the signal-to-noise ratio and enable detection of even smaller particles in which information on the morphology of nonspherical particles can be obtained by rotation of the excitation polarization with respect to the sample. The fact that our approach does not rely on the enhanced scattering cross section at that particular wavelength in order to reach adequate signal-to-noise ratios means that it is able to fully recover the amplitude and phase of light scattered by any small particle, and as such the technique has the potential to become a versatile tool for the study of the scattering properties of individual nanoparticles potentially even able to cross into a size regime where electromagnetism is no longer sufficient to describe particle-properties.[24] Moreover our moderate excitation powers will be essential to open up avenues to experimentally investigate the interaction between gold nanoparticles and single fluorescent molecules.[5]

In conclusion, we have experimentally demonstrated the feasibility of detecting metal nanoparticles down to 5 nm in size by interferometric cross-polarization microscopy. To achieve this we have combined conventional cross-polarized microscopy with optical heterodyne interferometry which efficiently amplifies the weak signal from individual nanoparticles enabling shot-noise-limited detection of the optical signal scattered by nanometer sized particles. Moreover our ability to measure the fields instead of intensity not only increases signal-to-noise but also enables retrieval of the full amplitude and phase response. With the intrinsic advantages of gold nanoparticles, such as nonphotobleaching

and unlimited lifetime and shape dependent optical response, our technique also has great potential for future application in biotechnology.

AUTHOR INFORMATION

Corresponding Author
*E-mail: h.gersen@bristol.ac.uk.

ACKNOWLEDGMENT

This work was funded in part by the Biotechnology and Biological Sciences Research Council through a Technology Development Research Initiative (Grant Ref: BB/F004494/1) and carried out with the support of the Bristol Centre for Nanoscience and Quantum Information. J.B.G. acknowledges support from the Royal Society (Grant Ref: NF082381), and N.F.v.H. acknowledges support of ICREA—Institució Catalana de Recerca i Estudis Avançats (Barcelona)

REFERENCES

(1) For a recent review see: Schuller, J. A.; Barnard, E. S.; Cai, W.; Jun, Y. C.; White, J. S.; Brongersma, M. L. *Nat. Mater.* **2010**, *9*, 193–204.
(2) For a recent review see: Shalaev, V. M. *Nat. Photonics* **2007**, *1*, 41–48.
(3) For a recent review see: Notomi, M. *Rep. Prog. Phys.* **2010**, *73*, No. 096501.
(4) Gersen, H.; Karle, T. J.; Engelen, R. J. P.; Bogaerts, W.; Korterik, J. P.; van Hulst, N. F.; Krauss, T. F.; Kuipers, L. *Phys. Rev. Lett.* **2005**, *94*, No. 073903.
(5) Trügler, A.; Hohenester, U. *Phys. Rev. B* **2008**, *77*, No. 115403.
(6) Arbouet, A.; Christofilor, D.; Fatti, N. D.; Vallée, F.; Huntzinger, J. R.; Arnaud, L.; Billaud, P.; Broyer, M *Phys. Rev. Lett.* **2004**, *93*, No. 127401.
(7) Ignatovich, F. V.; Novotny, L *Phys. Rev. Lett.* **2006**, *96*, No. 013901.
(8) Lindfors, K.; Kalkbrenner, T.; Stoller, P.; Sandoghdar, V. *Phys. Rev. Lett.* **2004**, *93*, No. 037401.
(9) Berciaud, S.; Cognet, L.; Blab, G. A.; Lounis, B. *Phys. Rev. Lett.* **2004**, *93*, No. 257402.
(10) Boyer, D.; Tamarat, P.; Maai, A.; Lounis, B.; Orrit, M. *Science* **2002**, *297*, 1160.
(11) Masia, F.; Langbein, W.; Watson, P.; Borri, P. *Opt. Lett.* **2009**, *34*, 1816.
(12) van Dijk, M. A.; Tchebotareva, A. L.; Orrt, M.; Lippitz, M.; Berciaud, S.; Lasne, D.; Cognet, L.; Lounis, B. *Phys. Chem. Chem. Phys.* **2006**, *8*, 3486.
(13) Berciaud, S.; Cognet, L.; Tamarat, P.; Lounis, B. *Nano Lett.* **2005**, *5*, 515.
(14) Muskens., O. L.; Billaud, P.; Broyer, M.; Del Fatti, N.; Vallée., F. *Phys. Rev. B* **2008**, *78*, No. 205410.
(15) Wilson, T.; Juskaitis, R.; Higdon, P. D. *Opt. Commun.* **1997**, *141*, 298.
(16) Bohren, C.; Huffman, D. *Absorption and Scattering of Light by Small Particles*; John Wiley & Sons: New York, 1983.
(17) Witteman, W. J. *Detection and Signal Processing: Technical Realization*; Springer: Berlin and Heidelberg, 2006; ISBN: 978-3-540-29599.
(18) Wilson, T.; Tan, J. B. *J. Microsc.* **1996**, *182*, 61.
(19) Balistreri, M. L. M.; Korterik, J. P.; Kuipers, L.; van Hulst, N. F. *J. Lightwave Technol.* **2001**, *19*, 1169.
(20) Mie, G. *Ann Phys.* **1908**, *25*, 377.
(21) Mojarad, N. M.; Zumofen, G.; Sandoghdar, V.; Agio, M. *J. Eur. Opt. Soc.—Rapid Publ.* **2009**, *4*, No. 09014.
(22) Novotny, L.; Hecht, B. *Principles of Nano-Optics*; Cambridge University Press: Cambridge and New York, 2006, ISBN: 978-0-521-83224-3.
(23) Gersen, H.; Garcia-Parajo, M. F.; Novotny, L.; Veerman, J. A.; Kuipers, L.; van Hulst, N. F. *Phys. Rev. Lett.* **2000**, *25*, 5312.
(24) Zheng, J.; Nicovich, P. R.; Dickson, R. M. *Annu. Rev. Phys. Chem.* **2007**, *58*, 409.